

## Article

# Effect of Lateral Trajectory on Two-Phase Flow in Horizontal Shale Gas Wells

Jian Yang, Jiaxiao Chen \*, Yang Peng and Bochun Li

Engineering Technology Research Institute, PetroChina Southwest Oil &amp; Gas Field Company, Chengdu 610017, China

\* Correspondence: chen\_jiavaxiao@126.com

**Abstract:** Horizontal gas wells are one of the key technologies for the production of shale gas reservoirs. Compared with conventional gas reservoirs, horizontal shale gas wells have ultra-long and complex lateral sections. Overall, toe-up, toe-down, and horizontal trajectories will be exhibited in the lateral section. The statistical results of field production data indicate that the lateral trajectory has a significant impact on the estimated ultimate recovery. However, the mechanism has not yet been fully revealed owing to the complicated two-phase flow in lateral pipes. Therefore, taking horizontal shale gas wells' lateral section as the research object, we designed our experimental parameter ranges based on horizontal shale gas wells in the Changning shale gas field. Simulation experimental tests were conducted on the pipe with an inclined angle from  $-15^\circ$  to  $15^\circ$  to analyze the effects of different gas velocities, liquid velocities, and pipe inclinations on flow patterns and liquid holdup. Based on our observations and measurements, we evaluated the flow pattern prediction methods and drew a new flow pattern map for pipes with an inclined angle from  $-15^\circ$  to  $15^\circ$ . Based on the momentum conservations between the gas and liquid phases and measured liquid holdup data, a new liquid holdup model was established in the pipes with inclined angle from  $-15^\circ$  to  $15^\circ$ . Experimental and field-measured data were collected to verify the new method's accuracy.

**Keywords:** horizontal shale gas well; lateral trajectory; two-phase flow; liquid holdup; flow pattern



**Citation:** Yang, J.; Chen, J.; Peng, Y.; Li, B. Effect of Lateral Trajectory on Two-Phase Flow in Horizontal Shale Gas Wells. *Processes* **2023**, *11*, 2844. <https://doi.org/10.3390/pr11102844>

Academic Editors: Mingjun Chen, Keliu Wu and Jiajia Bai

Received: 10 August 2023

Revised: 24 September 2023

Accepted: 26 September 2023

Published: 27 September 2023



**Copyright:** © 2023 by the authors. Licensee MDPI, Basel, Switzerland. This article is an open access article distributed under the terms and conditions of the Creative Commons Attribution (CC BY) license (<https://creativecommons.org/licenses/by/4.0/>).

## 1. Introduction

Shale gas development and the utilization of beneficial methods to alleviate the shortage of oil and gas resources are important supplements to conventional fossil fuels [1–3]. Horizontal well technology is commonly applied to drill shale gas reservoirs [4]. Compared with horizontal wells in conventional gas reservoirs, horizontal shale gas wells have an ultra-long horizontal section of 1000–3000 m and are affected by the vertical distribution of shale reservoirs, with typical toe-up and toe-down geometries exhibited in the lateral section. Meanwhile, the daily gas production of shale gas exhibits a hyperbolic decline, which is characterized by high initial gas production, rapid production decline, and a long low production cycle. As a shale gas well enters the late stage, the bottomhole flowing pressure significantly decreases, the production pressure difference decreases, and the gas-carrying capacity gradually decreases [5]. The gas well will produce with low gas production for a long time. Therefore, more and more studies focused on the two-phase flow in the wellbore throughout the horizontal gas wells' lifecycle [6,7]. On-site measured data on wellbore pressure show that ~75% of the loaded liquid is below the tubing shoes, indicating that, because of various factors such as the complex structure of the horizontal section, low gas production, and low pressure, some gas wells experience liquid being loaded in the lateral section [8]. Accurately predicting the flow behavior of the lateral section in horizontal gas wells has guiding significance for the implementation of deliquification technologies [9]. Regarding the liquid loading in horizontal wells, existing studies mostly focus on the vertical and inclined sections, while there is less research on the complex lateral trajectory effect on air–liquid two-phase flow behavior [10,11].

For horizontal or near-horizontal pipes, the model by Lockhart and Martinelli [12] initially introduced a distinct model for determining the frictional pressure gradient. Subsequently, Taitel and Dukler [13,14] devised one of the widely employed models for calculating pressure gradients and liquid holdup in horizontal and near-horizontal pipes. Their model assumes a stratified state with a flat interface, where the phases are segregated. To enhance the accuracy of these models, Hart et al. [15], Grolman and Fortuin [16], and Chen et al. [17] made modifications to the geometric distribution of the phases within the cross-sectional area. Al Safran [18] studied the slug flow characteristics in hilly-terrain pipelines within different superficial gas and liquid velocities, and inclination angles. He divided the slug flow state into five specific situations. According to Langsholt and Holm [19], the liquid holdup exhibited an abrupt increase with decreasing gas superficial velocities in pipe segments with slight inclinations ( $0.5^\circ$  to  $5^\circ$ ). In addition to comparing the effects of pipe inclination, water fraction, and system pressure, they also compared their results with those of the OLGAS 2000 commercial software. Fan et al. [20] employed two facilities in their experimental study with internal diameters of 0.05 m and 0.155 m. These facilities were inclined at angles ranging from  $\pm 2^\circ$  from the horizontal angle, and both air and water were used as flowing mediums. The researchers utilized a double-circle geometry and introduced a model for calculating the wetted wall fraction. Zhang and Sarica [21] extended Fan's model to unify the wetted wall fraction predictions and the transition to annular flow.

At lower gas flow rates in slightly inclined pipes, the flow behavior of low-liquid loading flows exhibits intermittent characteristics. The studies conducted by Alsaadi et al. [22], Fan et al. [23], and Fan et al. [24] investigated the initiation of liquid accumulation under inclinations ranging from  $2^\circ$  to  $30^\circ$  from the horizontal angle in a pipe with an inner diameter of 0.0762 m, using air and water as the flowing fluids. The experimental investigation by Arabi et al. [25] focused on the transition from a stratified to an intermittent air–water two-phase flow in a pipe with an inner diameter of 30 mm. Their study indicates that the onset of intermittent flow is primarily influenced by the liquid superficial velocity and the diameter of the pipe.

In recent years, some large-diameter and high-pressure experimental studies were conducted. Karami et al. [26] conducted a study on three-phase flow under low liquid loading in horizontal conditions using a low-pressure facility with an inner diameter of 0.155 m. Vuong et al. [27] investigated the effects of pressure on two-phase low liquid loading flow under high pressure ranging from 200 to 400 psig. The observed flow patterns were stratified wavy and annular flow, and various flow characteristics were measured, including liquid holdup, pressure gradients, wave characteristics, and wetted wall fractions. Rodrigues [28] conducted a study on pipes with slight inclinations, examining conditions similar to those investigated by Vuong with a  $2^\circ$  upward inclination. He proposed a novel model for estimating the gas–wall friction factor under stratified flow with a thin film present along the pipe, particularly at higher Froude numbers. Soedarmo [29] conducted an upward-inclined flow experiment in a high-pressure environment to analyze the effect of pressure on pattern transitions. Their experimental data demonstrated that the flow pattern boundaries move to the left under high-pressure conditions, compared with atmosphere-pressure conditions. As the pressure increased, the pseudo slug–slug transition gradually decreased. Farokhpour et al. [30] have scaled experiments with a diameter of 194 mm to a 44 mm diameter lateral pipe based on the principle of fluid density ratio. They found that, small-diameter pipelines exhibit a large-amplitude wave flow pattern compared to that with large-diameter pipelines at large liquid velocities.

To better understand the complex flow behavior in horizontal gas wells, we conducted gas–liquid pipe flow experiments to analyze the lateral geometry effect on flow behavior under different parameters. Based on the analysis of gas–liquid momentum conservation and experimental testing data, a prediction model for a near-horizontal section's liquid holdup was established, and a flow pattern map of a near-horizontal pipe was developed.

## 2. Experimental Facility

### 2.1. Flow Loop

The experimental tests were conducted in a new flow loop. The experimental facility adopts a visual plexiglass pipe to conduct experiments and observe the two-phase flow phenomenon. The pipe length is 8.6 m with a diameter of 114 mm, which is sufficient to fully develop the flow pattern when the fluid flows laterally along the pipeline. The pipe can be switched at any angle from  $-90^\circ$  to  $90^\circ$ , as shown in Figure 1.

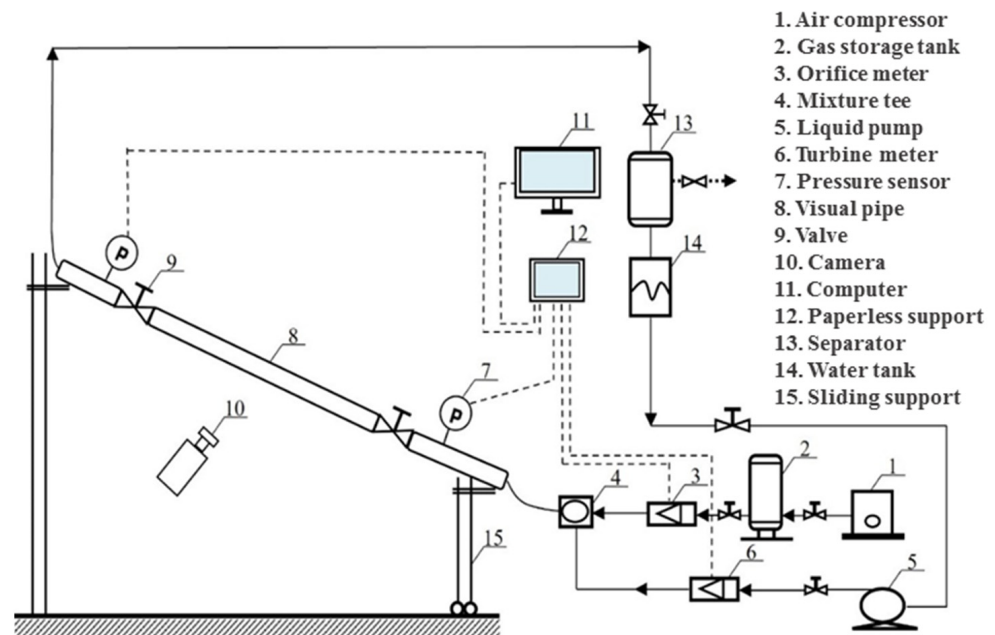


**Figure 1.** Experimental facility.

The whole experimental facility has three parts: a gas supply system, liquid supply system, and data acquisition system. The experimental fluids used are compressed air and tap water. Air is provided via a compressor and is stored in a gas tank and stably transported to the experimental tube section, while water is provided via a pump. All the measurement and test data are transmitted to the paperless recorder via the measuring instrument and then imported into the computer for data sorting and analysis. In addition, a gas–liquid separator is installed at the exit of the experimental device, and the gas is discharged into the air from the top of the separator, while the liquid is accumulated at the bottom of the separator for recycling. We measured liquid holdup by using two quick-closing ball valves under different experimental conditions to study gas–liquid flow characteristics. Flow behavior can be captured with a high-speed camera, and real-time pressure changes can be monitored with pressure sensors installed at the pipe ends; the specification of the experimental apparatus capabilities is in Table 1.

**Table 1.** Specification summary of the experimental apparatus capabilities.

Experimental Setup Components	Pressure Sensors	Orifice Meter	Turbine Meter
Accuracy, %	1.5	1.5	0.5

### 2.2. Test Matrix

Our experimental objective is to explore the lateral trajectory effect on the air–liquid flow pattern and liquid holdup, and thus provide some scientific knowledge and conclusions for production problems in horizontal shale gas wells. Therefore, this experimental campaign requires the establishment of experimental ranges suitable for horizontal shale gas wells. Consequently, we collected data from 88 typical horizontal shale gas wells from

the Changing shale gas field to determine our experimental ranges, which are listed in Table 2.

**Table 2.** Collected parameters from the horizontal wells of Changing shale gas field.

Data Number	Gas Flowrate $\times 10^4 \text{ m}^3/\text{d}$	Liquid Flowrate $\text{m}^3/\text{d}$	Casing Pressure MPa	Tubing Pressure MPa	Inclined Angle in Lateral Section
90	0.65–6.9	0.36–13	2.2–8.65	1.5–5.52	$-13^\circ$ – $15^\circ$

Between experimental studies under low-pressure conditions and gas wells under high-pressure conditions, flow pressure is one of the most important differences, as it could affect flow behavior entirely. Dimensionless numbers are often applied to characterize flow similarity in different situations when modeling flow behavior, which means different flow situations can be simulated similarly if proper dimensionless numbers are selected. Some scholars [31–33] have proposed new dimensionless numbers based on the modified Froude number in stratified and annular flows, and achieved high accuracy. The gas/liquid dimensionless numbers can be given as follows:

$$Fr_g = \sqrt{\frac{\rho_g}{\rho_l - \rho_g}} \frac{v_{sg}}{\sqrt{Dg \cos \theta}} \quad (1)$$

$$Fr_l = \sqrt{\frac{\rho_l}{\rho_l - \rho_g}} \frac{v_{sl}}{\sqrt{Dg \cos \theta}} \quad (2)$$

where  $Fr_g$  is the gas modified Froude number (dimensionless),  $Fr_l$  is the liquid modified Froude number (dimensionless),  $v_{sg}$  is the gas superficial velocity (in m/s),  $v_{sl}$  is the liquid superficial velocity (in m/s),  $D$  is the pipe diameter (in meters),  $\theta$  is the pipeline inclined angle (in degrees), and  $g$  is the gravitational acceleration (in  $\text{m}/\text{s}^2$ ).

We calculated the average flow pressures in the lateral section of this dataset and then converted these to those under our experimental conditions ( $20^\circ\text{C}$ ,  $0.101 \text{ MPa}$ ) based on the dimensionless numbers. Figure 2 presents the experimental ranges. It can be seen that  $v_{sg}$  and  $v_{sl}$  are  $0.5$ – $10 \text{ m/s}$  and  $0.0005$ – $0.02 \text{ m/s}$ , respectively. Therefore, our experimental ranges can be given based on these parameters, which are presented in Table 3.

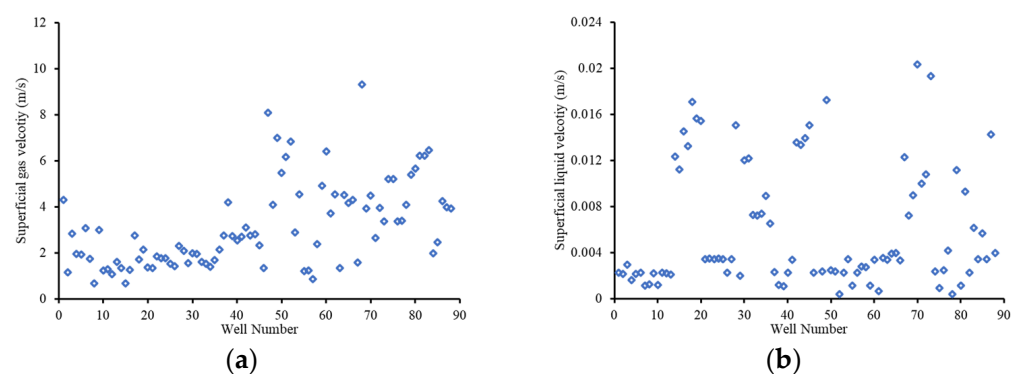


**Figure 2.** Converted experimental  $v_{sg}$  and  $v_{sl}$  based on the dimensionless numbers. (a)  $v_{sg}$  calculation; (b)  $v_{sl}$  calculation.

**Table 3.** Designed experimental parameters.

Pipe Diameter mm	Superficial Gas Velocity m/s	Superficial Liquid Velocity m/s	Inclined Angle
114	0.5, 1.5, 3, 4.5, 6, 8, 10	0.004, 0.008, 0.012, 0.016, 0.02	$-15^\circ$ , $-10^\circ$ , $-5^\circ$ , $0^\circ$ , $1^\circ$ , $5^\circ$ , $10^\circ$ , $15^\circ$

### 3. Experimental Results and Analysis

#### 3.1. Horizontal Pipe

##### 3.1.1. Effect of Superficial Gas Velocity

Figure 3 presents the observed flow behavior in a two-phase flow in a horizontal pipe ( $\theta = 0^\circ$ ) at different  $v_{sg}$  values when  $v_{sl}$  is 0.02 m/s. We can see that stratified flow is observed at different  $v_{sg}$  values, and as  $v_{sg}$  increases, the liquid film becomes thinner. When  $v_{sg}$  is 0.5 m/s, it is stratified smooth flow, and the liquid phase close to the lower pipe wall flows slowly and appears to be in a “stationary” state, with an obvious and smooth layering of the interface. When the gas superficial velocity increases to 4.5 m/s, small waves appear on the gas–liquid interface, and the flow becomes wavier. As  $v_{sg}$  further increases to 8 m/s, interfacial shear stress further increases, resulting in greater fluctuation and a thinner liquid film layer, which is consistent with the description of Chen et al. [17].

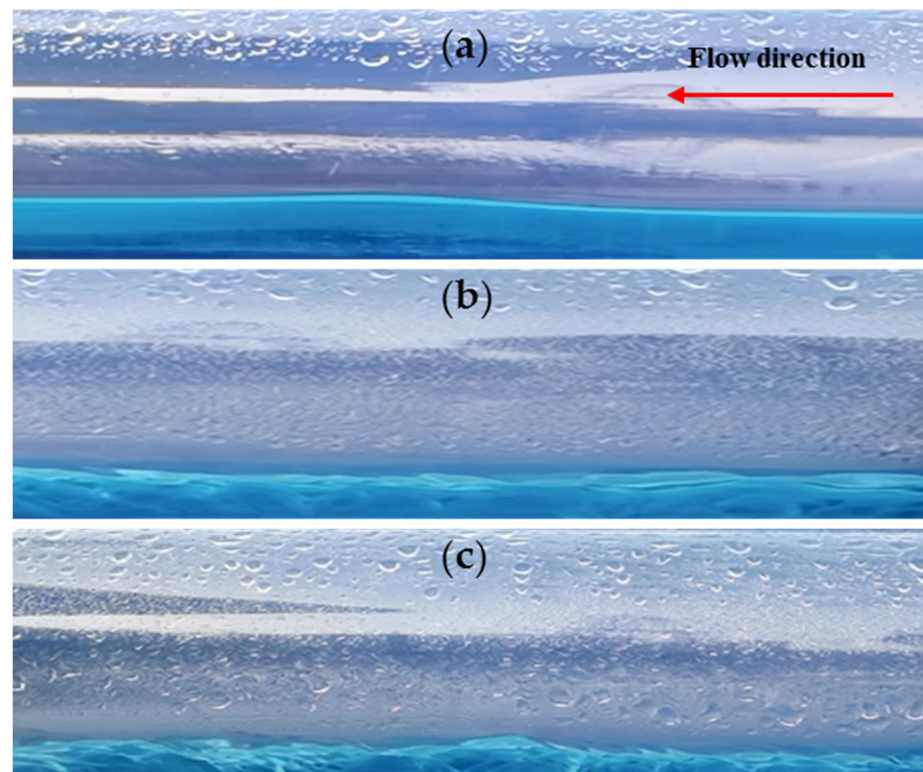


**Figure 3.** Snapshot of two-phase flow in a horizontal pipe at different  $v_{sg}$  values ( $v_{sl} = 0.02$  m/s). (a)  $v_{sg} = 0.5$  m/s; (b)  $v_{sg} = 4.5$  m/s; (c)  $v_{sg} = 8$  m/s.

##### 3.1.2. Effect of Superficial Liquid Velocity

Figure 4 presents the observed flow behavior in a horizontal pipe at different  $v_{sl}$  values when  $v_{sg}$  is 4.5 m/s. We can infer that, with the increase in  $v_{sl}$ , the liquid film becomes thicker and wavier. The flow pattern transitions from stratified smooth flow to stratified wavy flow.

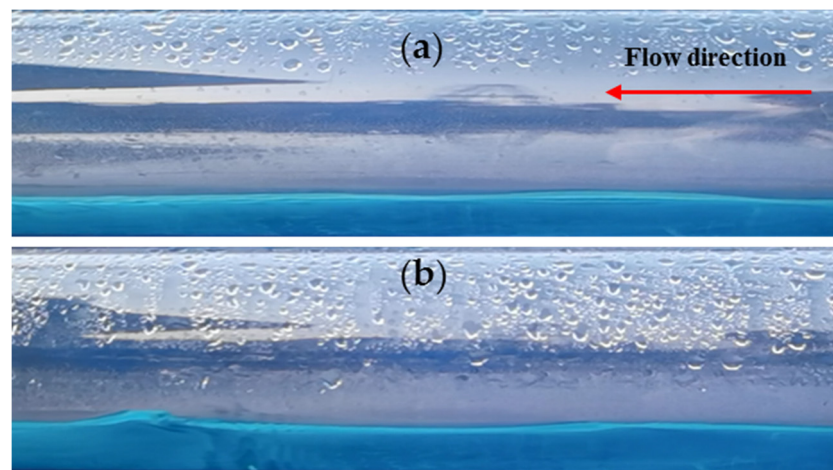


**Figure 4.** Snapshot of two-phase flow in a horizontal pipe at different  $v_{sl}$  values ( $v_{sg} = 4.5$  m/s). (a)  $v_{sl} = 0.012$  m/s; (b)  $v_{sl} = 0.02$  m/s.

### 3.2. Upward-Inclined Pipe

#### 3.2.1. Effect of Superficial Gas Velocity

Figure 5 presents the observed flow behavior in an upward-inclined pipe at different  $v_{sg}$  values when  $v_{sl}$  is 0.012 m/s and  $\theta$  is  $5^\circ$ . We can see the liquid will flow back and cause large liquid waves at a low  $v_{sl}$  value in an upward-inclined pipe, which is totally different from the flow behavior in a horizontal pipe. When  $v_{sg}$  is 0.5 m/s, it can be observed that liquid bridges the pipe, indicating the appearance of liquid slugs, which is consistent with the observation of Nair [34] and Arabi et al. [35] and this is the reason for pressure fluctuations and severe slugging. With the increase in  $v_{sg}$ , the liquid slug will gradually disappear and stable stratified flow will be reached at  $v_{sg} = 10$  m/s.

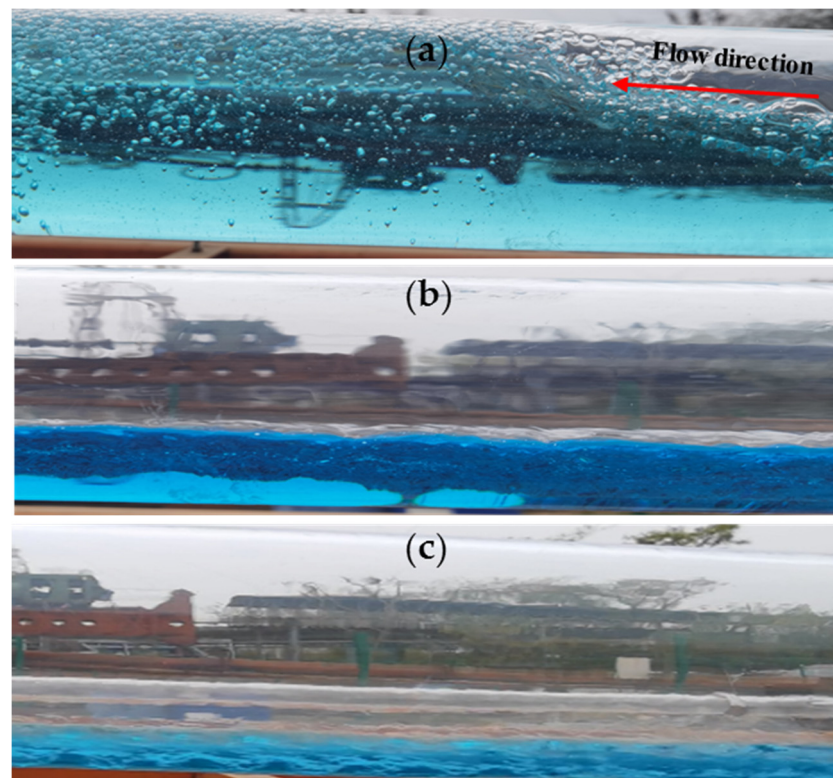


**Figure 5.** Snapshot of two-phase flow in an upward-inclined pipe at different  $v_{sg}$  values ( $v_{sl} = 0.012$  m/s,  $\theta = 5^\circ$ ). (a)  $v_{sg} = 0.5$  m/s; (b)  $v_{sg} = 6$  m/s; (c)  $v_{sg} = 10$  m/s.

### 3.2.2. Effect of Superficial Liquid Velocity

Figure 6 presents the observed flow behavior in an upward-inclined pipe at different  $v_{sl}$  values when the  $v_{sg}$  is 3 m/s and  $\theta$  is  $5^\circ$ . With the increase in  $v_{sl}$ , higher interfacial stress will be required to drag the liquid upward. Therefore, at the same  $v_{sg}$  value, the flow with a higher  $v_{sl}$  value will flow back more easily and thus larger liquid slugs and fluctuations will form. When  $v_{sl}$  reaches 0.02 m/s, we can see liquid bridge the pipe totally, which is very different from the phenomenon at  $v_{sl} = 0.004$  m/s. The flow pattern changes from stratified flow at  $v_{sl} = 0.004$  m/s to slug flow at  $v_{sl} = 0.02$  m/s.

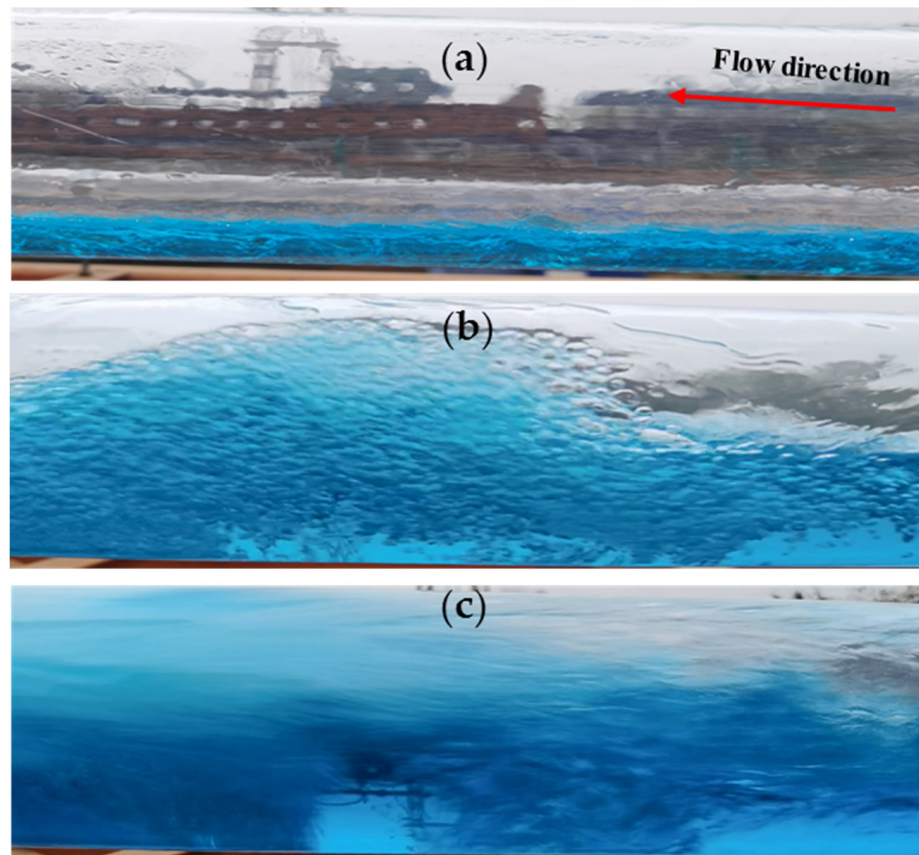


**Figure 6.** Snapshot of two-phase flow in an upward-inclined pipe at different  $v_{sl}$  values ( $v_{sg} = 3$  m/s,  $\theta = 5^\circ$ ). (a)  $v_{sl} = 0.004$  m/s; (b)  $v_{sl} = 0.016$  m/s; (c)  $v_{sl} = 0.02$  m/s.

### 3.2.3. Effect of the Inclined Angle

Figure 7 presents the observed flow behavior in an upward-inclined pipe at different inclined angles when  $v_{sg}$  is 3 m/s and  $v_{sl}$  is 0.012 m/s. With the increase in the inclined angle, it is obvious that the liquid film can more easily flow back as a result of the influence of gravity and that oscillation increases in amplitude. When the inclined angle is  $15^\circ$ , it can be seen that liquid slugs will pass through the pipe periodically.

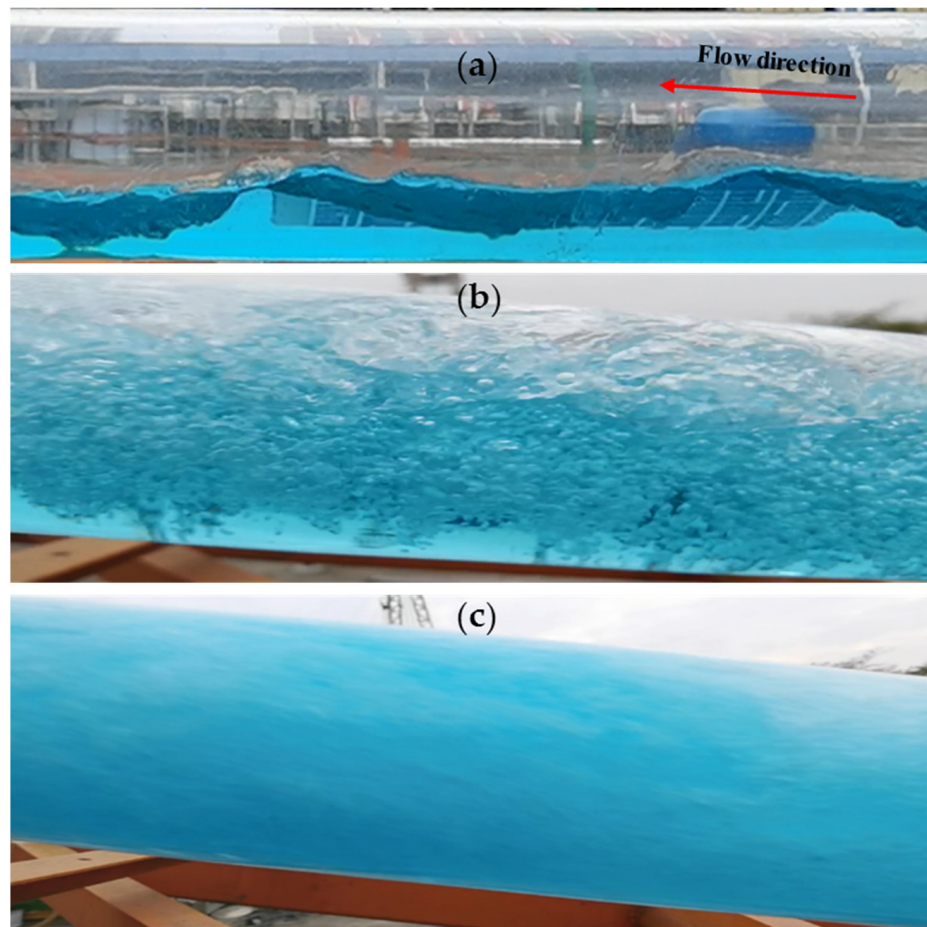


**Figure 7.** Snapshot of two-phase flow in an upward-inclined pipe at different inclined angles ( $v_{sg} = 3$  m/s,  $v_{sl} = 0.012$  m/s). (a)  $\theta = 1^\circ$ ; (b)  $\theta = 10^\circ$ ; (c)  $\theta = 15^\circ$ .

### 3.3. Downward-Inclined Pipe

For downward flow, the flow behavior is much simpler. We can see that the flow pattern will exhibit stratified flow under different conditions, as shown in Figure 8. With the increase in the inclined angle, the liquid film thickness decreases. This is because liquid film is mainly affected by gravity and the shear stress force at the gas–liquid interface, and the gravity force as the driving force increases with the increase in  $\theta$ . Therefore, the liquid film velocity on the pipe wall increases with the increase in  $\theta$ .

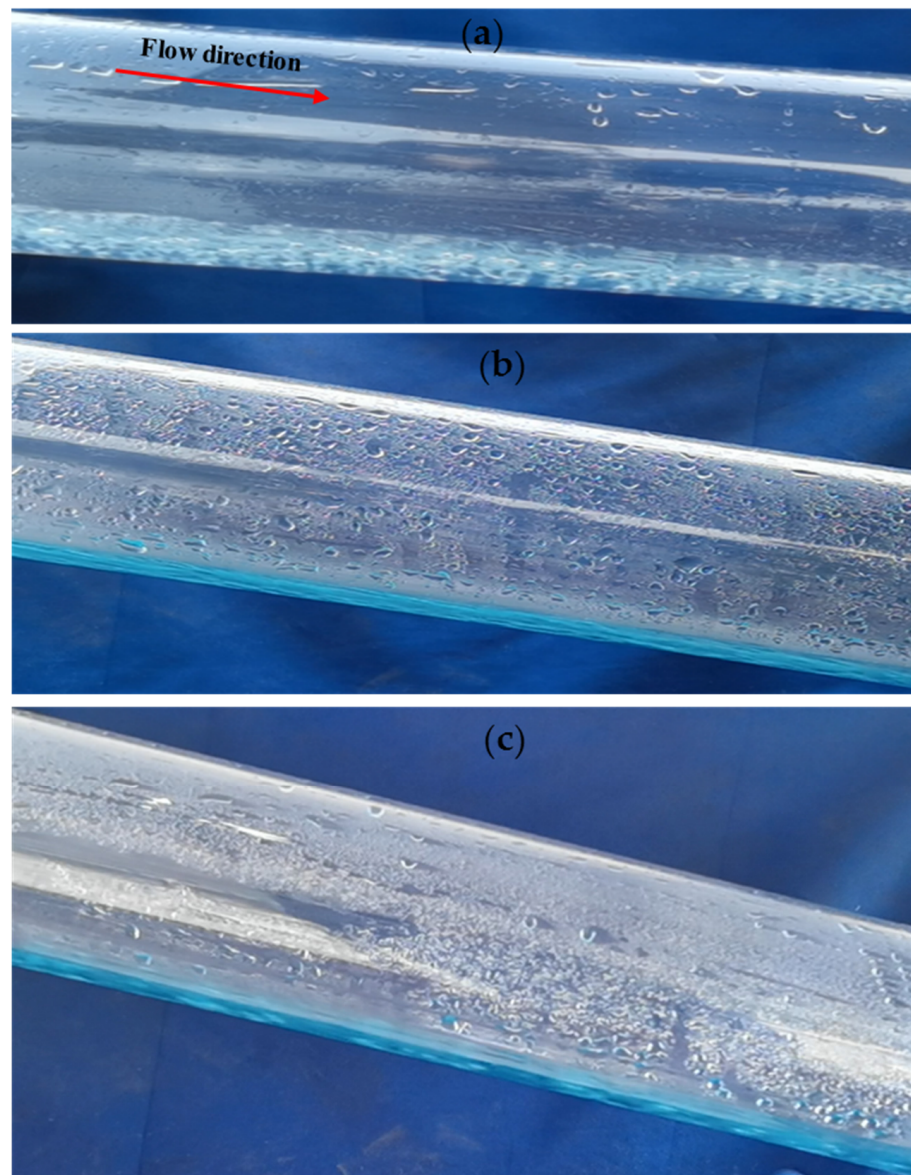


**Figure 8.** Snapshot of two-phase flow in a downward pipe under different conditions. (a)  $v_{sg} = 4.5$  m/s;  $v_{sl} = 0.012$  m/s;  $\theta = -5^\circ$ ; (b)  $v_{sg} = 6$  m/s;  $v_{sl} = 0.01$  m/s;  $\theta = -10^\circ$ ; (c)  $v_{sg} = 0.5$  m/s;  $v_{sl} = 0.02$  m/s;  $\theta = -15^\circ$ .

#### 4. Flow Pattern Evaluation and Establishment

Our experimental observation suggest that the inclined angle has a significant impact on flow patterns. Therefore, flow pattern maps in near-horizontal pipes must take the inclined angle into account. In horizontal pipes, according to their authors, the Mandhane map is commonly applied to deal with the flow pattern, and it remains applicable to the case with a pipe diameter of  $>100$  mm [36]. Because the flow pattern is greatly affected by the inclined angle, there is no unique flow pattern at a certain inclined angle, and predicting existing flow maps is difficult for all inclined angles. Therefore, we use the mechanistic approach established by Zhang et al. [37] to deal with the pattern in upward-/downward-inclined pipes.

Figure 9 shows the prediction using the Mandhane flow pattern map. We observed stratified smooth and wavy flows at  $v_{sl}$  from 0.004 to 0.2 m/s in a horizontal pipe. However, the lowest  $v_{sl}$  in the Mandhane flow pattern map is 0.01 m/s, which means that this flow pattern cannot be used to deal with the flow pattern in some horizontal wells with a low  $v_{sl}$  value. Furthermore, we can see that the Mandhane map cannot accurately predict pattern

transitions. This might be caused by the different pipe sizes between our experiment and those used to construct the Mandhane flow pattern map.

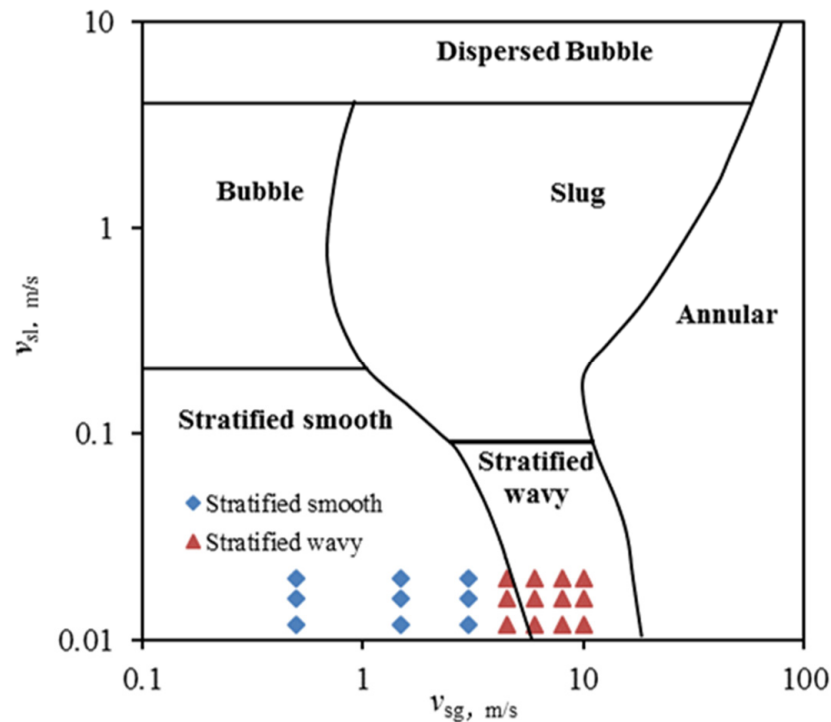


**Figure 9.** Evaluation results from the horizontal pipe against those with the Mandhane map.

The evaluation results in the upward-inclined pipe against those under the Zhang et al. model are presented in Figure 10. We can see that the flow pattern is greatly affected by the inclined angle. With the increase in the inclined angle, non-annular flow will occur more easily. As can be seen, the Zhang model recognizes more annular flows as non-annular flows, especially when the inclined angle is  $10^\circ$  and  $15^\circ$ .

In a downward-inclined pipe, flow behavior is relatively steady and it presents as stratified flow at different inclinations. As presented in Figure 11, the inclined angle has a minor effect at low superficial liquid velocities according to the Zhang et al. model. In our experimental ranges, we can see that the Zhang et al. model predicts an accurate stratified flow at all of the points.

In summary, we can infer that the existing flow pattern maps and mechanistic models are not accurate in predicting the flow patterns at different angles. Therefore, according to our observation, we established a new flow pattern map considering the inclination, which is more suitable for horizontal gas well production ranges. The new map takes  $v_{sg}$  and  $v_{sl}$  as the coordinates, respectively, as is shown in Figure 12. In this map, non-annular flow and annular flow are recognized. Note that annular flow will be present under different conditions when the inclined angle is lower than  $1^\circ$ . We can also see from this figure that, as the inclination increases, the transition boundary moves significantly to the right, indicating that the stratified flow area gradually decreases. The required  $v_{sg}$  for the transition from non-annular to annular flow increases with the increase in inclination and  $v_{sl}$ . Note that only stratified flow will be present for horizontal and downward-inclined pipes.

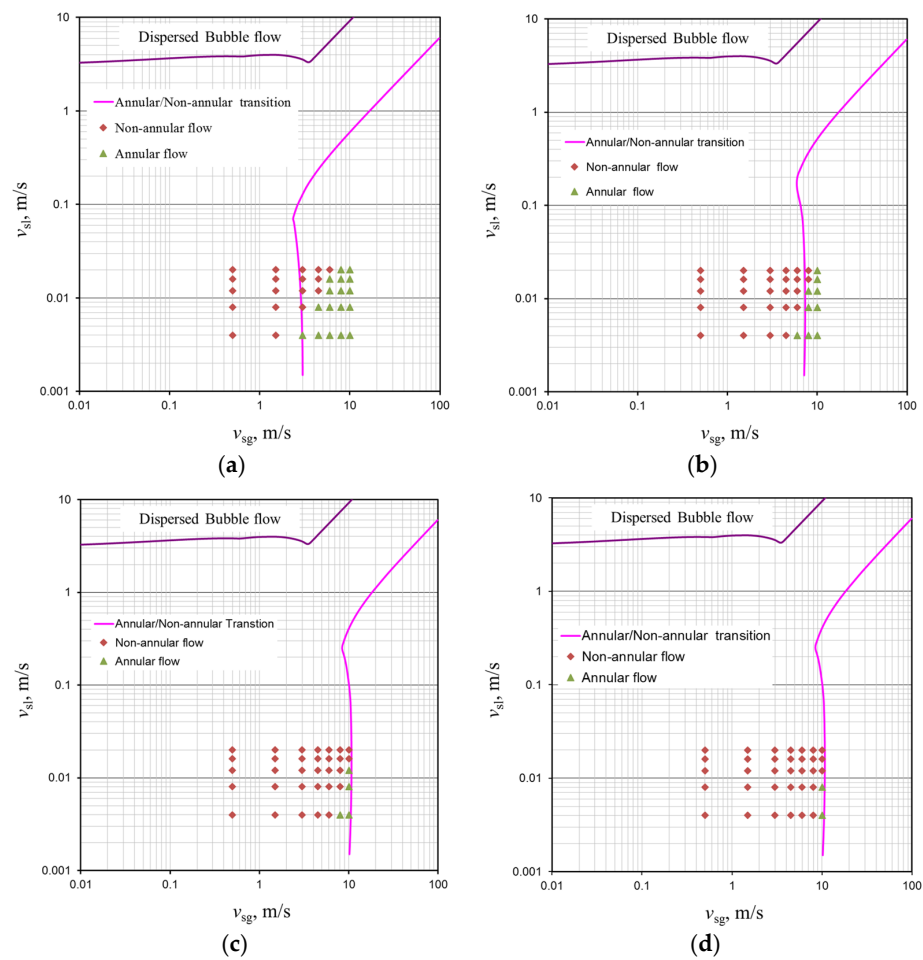


**Figure 10.** Evaluation results for the upward-inclined pipe against those under the Zhang et al. model. (a) 1°; (b) 5°; (c) 10°; (d) 15°.

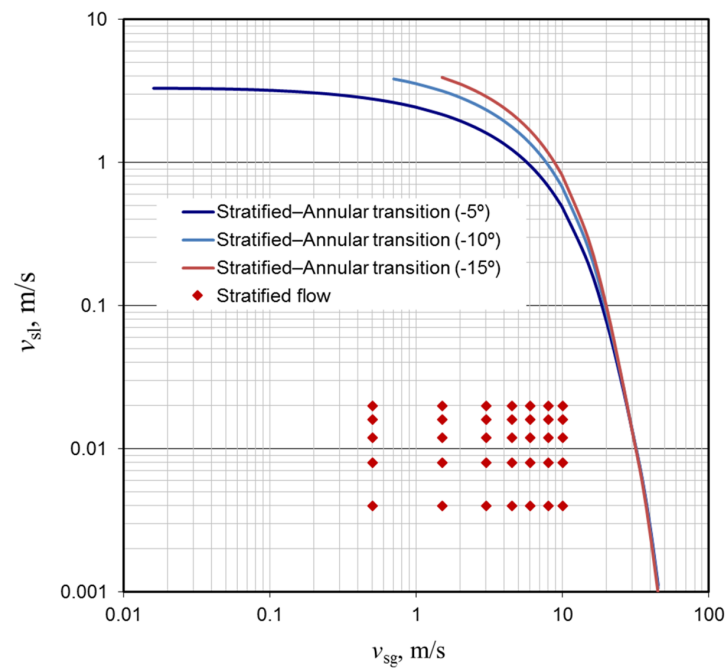


**Figure 11.** Evaluation results for the downward-inclined pipe against those under the Zhang et al. model.

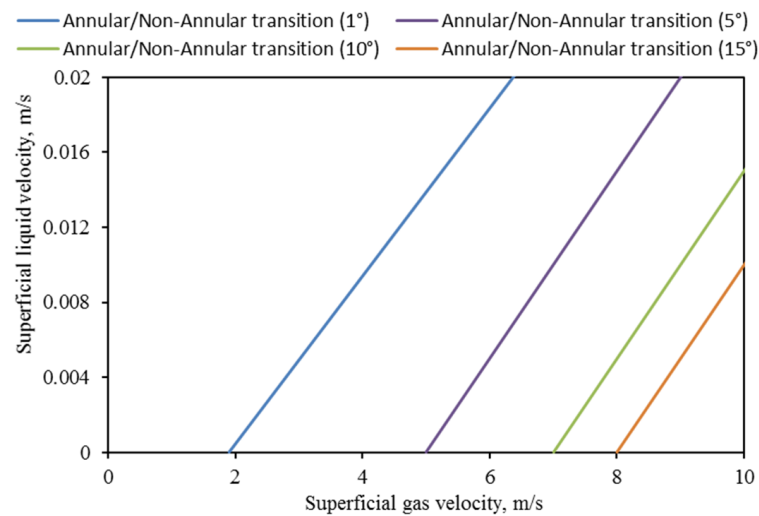
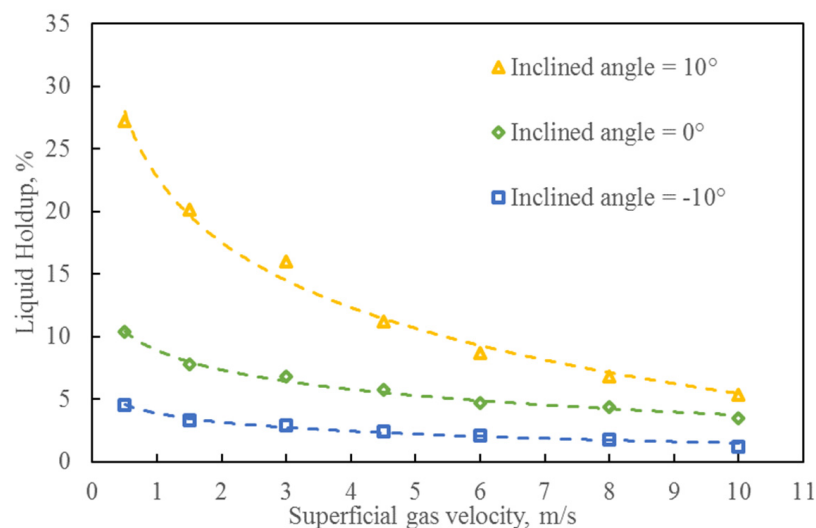


**Figure 12.** New flow pattern map with inclined angle from  $-15^\circ$  to  $15^\circ$ .

## 5. Liquid Holdup Model Establishment

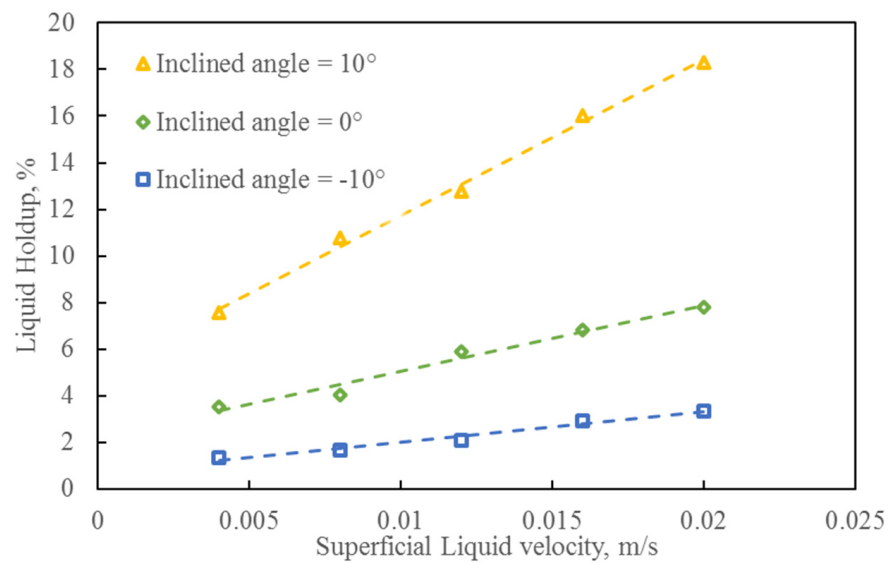
### 5.1. Liquid Holdup Analysis

Figure 13 shows the liquid holdup variation with  $v_{sg}$  at different lateral trajectories when  $v_{sl}$  is 0.016 m/s. The liquid holdup in a downward-inclined pipe is lowest among the three trajectories, which is much more obvious at a low  $v_{sg}$ . This is consistent with our observation. In a downward-inclined flow, liquid can flow downward spontaneously due to the force of gravity without a drag force from the gas. Consequently, there will be much less slippage between the gas and liquid. For an upward-inclined flow, the curve is steeper when  $v_{sg}$  is  $< 5$  m/s. This is because, with a decrease in  $v_{sg}$ , the liquid phase gradually turns from being in a discontinuous phase to being in a continuous one. When the liquid phase is continuous and the gas phase is discontinuous, the liquid is more likely to load in the wellbore and a slight decrease in gas velocity will cause a rapid increase in liquid holdup.



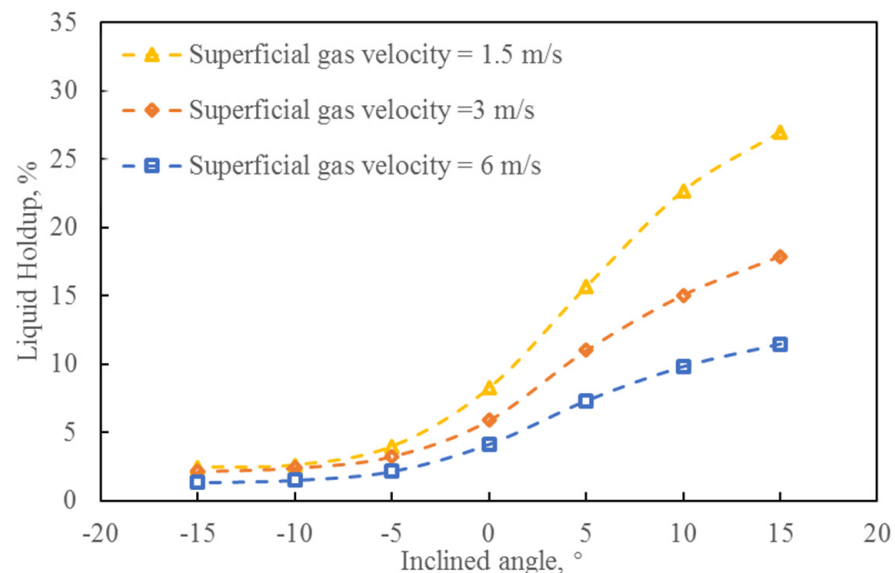
**Figure 13.** Variation in liquid holdup with  $v_{sg}$  at different lateral trajectories ( $v_{sl} = 0.016$  m/s).

Figure 14 presents the liquid holdup variation with  $v_{sl}$  at different lateral trajectories when  $v_{sg}$  is 3 m/s. As  $v_{sl}$  increases, liquid holdup increases at different lateral trajectories, and the increase is greatest in an upward-inclined pipe. This is because more liquid will flow in the pipe and occupy a greater area. We can also infer that liquid holdup has a linear relationship with the superficial liquid velocity.



**Figure 14.** Variation in liquid holdup with superficial liquid velocity at different lateral trajectories ( $v_{sg} = 3$  m/s).

Figure 15 presents the liquid holdup variation with the inclined angle at different  $v_{sg}$  values when  $v_{sl}$  is 0.012 m/s. As the inclined angle gradually increases, the pipe trajectory changes from being downward-inclined to upward-inclined and the liquid holdup has a totally different trend. We can see that the liquid holdup increases slowly in a downward-inclined pipe and then increases rapidly in an upward-inclined pipe. This is because when the pipe is inclined upwards, liquid will easily flow back due to gravity. Especially at a low superficial gas velocity, much liquid accumulates and causes large liquid waves, thus increasing liquid holdup rapidly.



**Figure 15.** Variation in liquid holdup with inclined angle at different  $v_{sg}$  values ( $v_{sl} = 0.012$  m/s).

## 5.2. Model Establishment

Based on our observations and measurements above, we can infer that it is difficult to model liquid holdup based on the momentum conservation of a liquid/gas in upward-inclined pipes because the interface changes rapidly with the inclined angle. For a better prediction of the liquid holdup under an inclined angle from  $15^\circ$  to  $15^\circ$ , we propose a new method to model liquid holdup variation with gas and liquid velocities and inclinations.

For horizontal pipes, we established a liquid holdup model based on force balance; we then correlated the liquid holdup at different inclined angles with the experimental results.

A force analysis diagram for gas and liquid is presented in Figure 16. The momentum conservation equation for a two-phase flow can be given and follows Taitel and Dukler [14]:

$$-A_g \frac{dp}{dx} - \tau_{wg} S_g - \tau_i S_i = 0 \quad (3)$$

$$-A_l \frac{dp}{dx} - \tau_{wl} S_l + \tau_i S_i = 0 \quad (4)$$

where  $A_g$  is the cross-sectional area covered by the gas (in  $m^2$ ),  $A_l$  is the cross-sectional area covered by the liquid (in  $m^2$ ),  $\tau_{wg}$  is the shear force between the gas phase and the pipe wall (in pascals),  $\tau_{wl}$  is the shear force between the liquid phase and the pipe wall (in pascals),  $\tau_i$  is the interfacial shear stress (in pascals),  $p$  is the pressure (in pascals),  $x$  is the pipe length (in meters),  $S_g$  is the gas phase's wet circumference (in meters),  $S_l$  is the liquid phase's wet circumference (in meters), and  $S_i$  is the length of the gas–liquid interface at the cross-section of the pipeline (in meters).

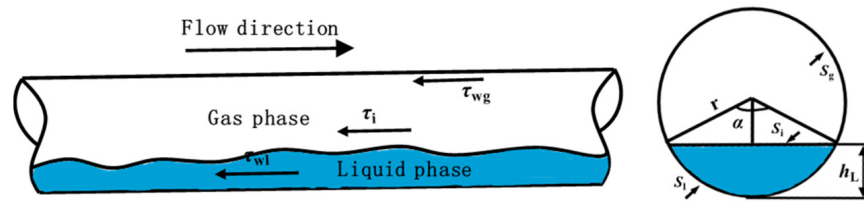


**Figure 16.** Schematic of stratified flow in a horizontal pipe.

Note that the pressure gradient terms in the two-phase momentum conservation equations are equal. Therefore, the combined equation can be obtained by eliminating the pressure gradient terms in Equations (3) and (4), and we can obtain

$$\tau_{wl} \frac{S_l}{A_l} - \tau_{wg} \left[ \frac{S_g}{A_g} + \frac{\tau_i}{\tau_{wg}} \left( \frac{S_i}{A_g} + \frac{S_i}{A_l} \right) \right] = 0 \quad (5)$$

In the above equation,  $\tau_{wg}$ ,  $\tau_{wl}$ , and  $\tau_i$  can be expressed as follows:

$$\tau_{wg} = f_{wg} \frac{\rho_g v_g^2}{2} \quad (6)$$

$$\tau_{wl} = f_{wl} \frac{\rho_l v_l^2}{2} \quad (7)$$

$$\tau_i = f_i \frac{\rho_g (v_g - v_l)^2}{2} \quad (8)$$

where  $f_{wg}$  is the gas friction factor (dimensionless),  $f_{wl}$  is the liquid friction factor (dimensionless), and  $f_i$  is the interfacial friction factor (dimensionless).

$f_{wg}$  and  $f_{wl}$  can be calculated from the Blasius equation:

$$f_{wg} = 0.079 \text{Re}_g^{-0.25} \quad (9)$$

$$f_{wl} = 0.079 \text{Re}_l^{-0.25} \quad (10)$$

where the Reynolds numbers of gas and liquid in Equations (9) and (10) are calculated as follows:

$$\text{Re}_g = \rho_g D v_g / \mu_g \quad (11)$$

$$\text{Re}_l = \rho_1 D v_1 / \mu_1 \quad (12)$$

For pipe diameters of <127 mm and considering the flow pattern transition in horizontal pipes, Andritsos and Hanratty [38] suggested using the critical superficial gas velocity,  $v_{\text{sgt}}$ , from a laminar to a wavy flow as the criterion for determining the interfacial friction factor,  $f_i$ . The  $f_i/f_{\text{wg}}$  relationship is then obtained as follows:

$$\frac{f_i}{f_{\text{wg}}} = 1, \quad v_{\text{sg}} \leq v_{\text{sgt}} \quad (13)$$

$$\frac{f_i}{f_{\text{wg}}} = 1 + 15 \sqrt{\frac{h_L}{D}} \left( \frac{v_{\text{sg}}}{v_{\text{sgt}}} - 1 \right), \quad v_{\text{sg}} > v_{\text{sgt}} \quad (14)$$

The critical superficial gas velocity can be obtained from

$$v_{\text{sgt}} = 5 \sqrt{\frac{101325}{p}} \quad (15)$$

and the geometric parameters are given as follows:

$$D_g = \frac{4A_g}{S_g + S_i} \quad (16)$$

$$D_1 = \frac{4A_1}{S_1} \quad (17)$$

$$S_g = \cos^{-1} \left( 2 \frac{h_L}{D} - 1 \right) \quad (18)$$

$$S_1 = \pi - \cos^{-1} \left( 2 \frac{h_L}{D} - 1 \right) \quad (19)$$

$$S_i = \sqrt{1 - \left( 2 \frac{h_L}{D} - 1 \right)^2} \quad (20)$$

$$A_g = 0.25 \left[ S_g - S_i \left( \frac{2h_L}{D} - 1 \right) \right] \quad (21)$$

$$A_1 = 0.25 (\pi - 4A_g) \quad (22)$$

The above geometric parameters are all related to  $h_L/D$ , so Equation (5) can be expressed as  $h_L/D$  as follows:

$$F \left( \frac{h_L}{D} \right) = 0 \quad (23)$$

Based on the geometric relationship, the liquid holdup,  $H_{L(0)}$ , of the horizontal pipe can be calculated as follows:

$$H_{L(0)} = \frac{\alpha - \sin \alpha}{2\pi} \quad (24)$$

$$\alpha = \cos^{-1} \left( 1 - 2 \frac{h_L}{D} \right) \quad (25)$$

The liquid holdup prediction model above is only applicable to horizontal pipes. For inclined pipes, the change in angle complicates the flow pattern transitions and liquid holdup, and it is difficult to define the flow pattern transformation point and predict liquid holdup. Beggs and Brill [39] established an empirical relationship between the inclination

correction coefficient and the angle based on liquid holdup data from a horizontal section measured experimentally, thereby characterizing the effect of the inclined angle on liquid holdup. Mukherjee et al. [40] and Lou et al. [41] directly consider the inclined angle as a polynomial of the sine function. Luo et al. [42] and Liu et al. [43] established a power-law curve to predict the liquid holdup in a vertical pipe and a corresponding angle correlation term. In conclusion, the liquid holdup of an inclined pipe can be predicted by using the liquid holdup in a horizontal pipe according to the relationship between the liquid holdups of inclined and horizontal pipes at different angles under the same conditions. The regression of the existing models is based on a wide fluid flow range, and the predictability is poor for the low-production fluid flow of horizontal shale gas wells. Therefore, based on the angle correction term, in this study, we proposed a liquid holdup model for near-horizontal pipes. The model was developed based on the liquid holdup in horizontal pipes and is given as follows:

$$H_{L(\theta)} = H_{L(0)} \left( 1 + a \sin^3 \theta + b \sin^2 \theta + c \sin \theta \right) \quad (26)$$

where  $H_{L(\theta)}$  is the liquid holdup of an inclined pipe (in percent) and  $a$ ,  $b$ , and  $c$  are the fitting coefficients.

Based on the experimental testing of liquid holdup data in this study, parameter fitting was performed for Equation (26), and the fitting model for inclined pipe liquid holdup was obtained as follows:

$$H_{L(\theta)} = H_{L(0)} \left( 1 - 32.56 \sin^3 \theta + 7.04 \sin^2 \theta + 10.08 \sin \theta \right) \quad (27)$$

Figure 17 shows the comparison between the predicted liquid holdup and the measured liquid holdup of the new model at different superficial gas and liquid velocities, from which it can be seen that the new model has good performance in predicting the liquid holdup under different flow conditions, with an average percentage error of  $-1.09\%$  and an average absolute error of  $7.61\%$ .

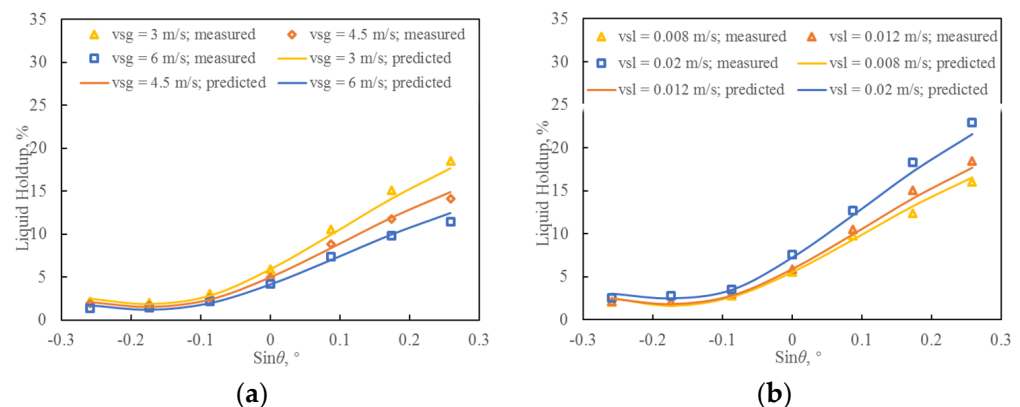


**Figure 17.** Comparison of measured and predicted results. (a)  $v_{sl} = 0.012$  m/s; (b)  $v_{sg} = 3$  m/s.

### 5.3. Model Validation

To better evaluate the new model's performance, we validated it with our experimental tests and some experimental data from the literature. For comparison, some widely used models, namely the Beggs–Brill model, the Eaton model [44], and the Xiao model [45], were also evaluated.

Model performance was evaluated based on the average percentage relative error, average percentage absolute error, and standard percentage error. The average percentage

relative error,  $E_1$ , represents the overall deviation of the model's prediction results, and the calculation formula is as follows:

$$E_1 = \frac{1}{n} \sum_{i=1}^n \frac{p_{ci} - p_{ti}}{p_{ti}} \times 100\% \quad (28)$$

The average percentage absolute error,  $E_2$ , indicates the size of the average error in the model prediction results, which is given as

$$E_2 = \frac{1}{n} \sum_{i=1}^n \left| \frac{p_{ci} - p_{ti}}{p_{ti}} \right| \times 100\% \quad (29)$$

The standard percentage error,  $E_3$ , represents the degree of dispersion of the model's calculation results as follows:

$$E_3 = \sqrt{\frac{1}{n-1} \sum_{i=1}^n \left( \frac{p_{ci} - p_{ti}}{p_{ti}} - E_1 \right)^2} \times 100\% \quad (30)$$

In total, 84 sets of experimental test liquid holdup data were collected in our experiment. Figure 18 shows the models' accuracy. It can be inferred that the new model has the best performance among all four models, having  $E_1$ ,  $E_2$ , and  $E_3$  values of  $-2.15\%$ ,  $7.46\%$ , and  $8.86\%$ , respectively.

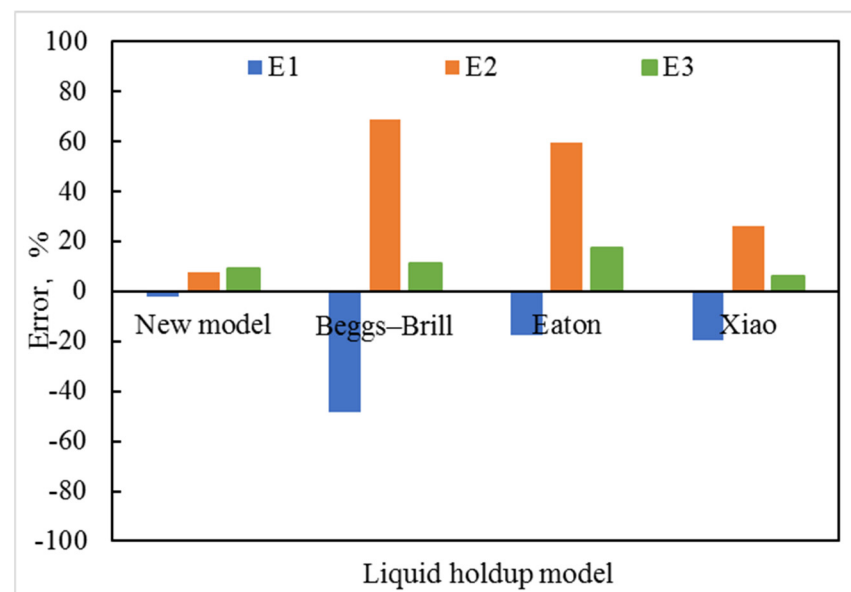
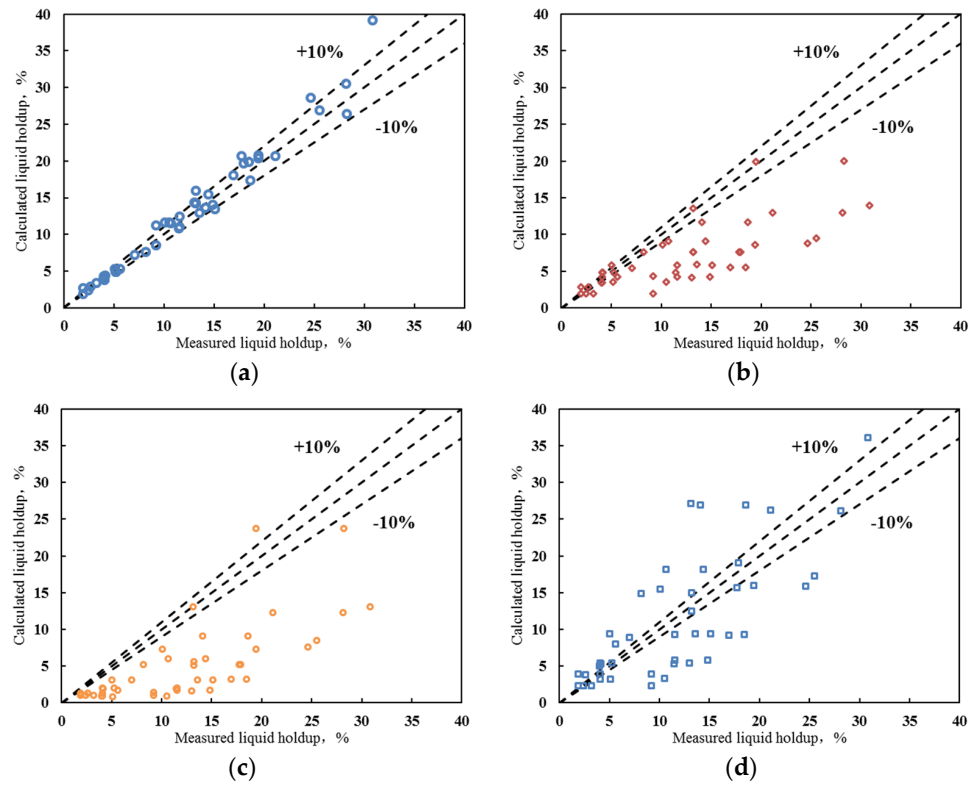


**Figure 18.** Model validation against our experiment results.

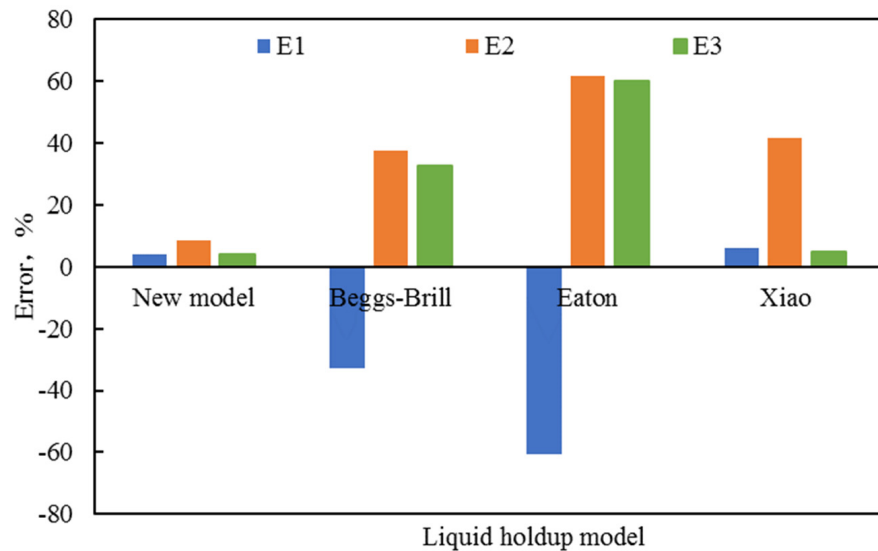
Because our new model for inclined pipes was retrieved from experimental data, it might increase accuracy when validated with our dataset. Therefore, we collected another dataset from Alsaadi [22], which has 46 data points. These experimental data were obtained from a 76.2 mm diameter pipe with a length of 17.7 m and superficial liquid velocities ranging from 0.01 to 0.05 m/s.

Figure 19 shows the measured liquid holdup variation with the predicted liquid holdup obtained using these four models. We can see that almost all data points fall within the 10% error line in the new model and that these points are more evenly distributed compared to those of other models. The Beggs-Brill and Eaton models underestimated the prediction of liquid holdup, resulting in severe deviations and exceeding the error range of most data point distributions, while the Xiao model predicted a more dispersed distribution of points. Overall, the new model has an  $E_1$  of 4.19%,  $E_2$  of 8.68%, and  $E_3$  of 4.10%, as

shown in Figure 20. These results indicate that the prediction accuracy of the new model is significantly better than that of other models involved in the comparative evaluation.



**Figure 19.** Comparison of the model-predicted liquid holdup and the measured liquid holdup. (a) new model; (b) Beggs-Brill model; (c) Eaton model; (d) Xiao model.



**Figure 20.** Model validation against the Alsaadi dataset.

**6. Conclusions**

- (1) The widely used flow pattern prediction methods have low accuracy in predicting flow patterns in near-horizontal pipes based on our experimental observation. We developed a new flow pattern map considering the effect of an inclined angle that is more suitable for predicting flow patterns in horizontal shale gas wells.
- (2) The liquid holdup of downward-inclined pipes is less affected by changes in flow parameters, while the liquid holdup of horizontal and upward-inclined pipes decreases

rapidly, then slows down with an increase in the superficial gas velocity and increases linearly with an increase in superficial liquid velocity. With an increase in the inclined angle, liquid holdup slowly increases at first and then increases rapidly.

- (3) A near-horizontal liquid holdup prediction model was established based on the force analysis between gas and liquid phases and the experimental results. Experimental data and literature data were used to evaluate the prediction accuracy of the model. The average percentage relative errors were  $-2.15\%$  and  $4.19\%$ , respectively. The new model's prediction accuracy was higher than that of other models involved in the comparative evaluation, indicating the reliability of the model.

**Author Contributions:** Conceptualization, J.Y. and J.C.; methodology, J.Y. and J.C.; software, Y.P. and B.L.; validation, B.L.; formal analysis, J.C.; investigation, Y.P.; resources, J.Y.; writing—original draft preparation, J.Y. and B.L.; writing—review and editing, J.Y. and J.C.; visualization, J.C.; supervision, Y.P.; project administration, J.Y.; funding acquisition, Y.P. All authors have read and agreed to the published version of the manuscript.

**Funding:** This research was funded by Science and Technology Cooperation Project of the CNPC-SWPU Innovation Alliance (grant no. 2020CX020203).

**Data Availability Statement:** The data that support the findings of this study can be provided by the corresponding author upon reasonable request.

**Conflicts of Interest:** The authors declare no conflict of interest.

## References

1. Yang, J.; Wang, Q.; Sun, F.; Zhong, H.; Yang, J. Simulation Experiment and Mathematical Model of Liquid Carrying in the Entire Wellbore of Shale Gas Horizontal Wells. *Processes* **2023**, *11*, 2339. [[CrossRef](#)]
2. Luo, C.; Cao, Y.; Liu, Y.; Zhong, S.; Zhao, S.; Liu, Z.; Liu, Y.; Zheng, D. Experimental and modeling investigation on gas-liquid two-phase flow in horizontal gas wells. *J. Energy Resour. Technol.* **2022**, *145*, 013102. [[CrossRef](#)]
3. Cheng, Y.; Wu, R.; Liao, R.; Liu, Z. Study on Calculation Method for Wellbore Pressure in Gas Wells with Large Liquid Production. *Processes* **2022**, *10*, 685. [[CrossRef](#)]
4. Luo, C.; Gao, L.; Liu, Y.; Xie, C.; Ye, C.; Yang, J.; Liu, Z. A modified model to predict liquid loading in horizontal gas wells. *J. Energy Resour. Technol.* **2023**, *145*, 083502. [[CrossRef](#)]
5. Browning, S.; Jayakumar, R. Effects of Toe-Up Vs Toe-Down wellbore trajectories on production performance in the Cana Woodford. In Proceedings of the Unconventional Resources Technology Conference, San Antonio, TX, USA, 1–2 August 2016.
6. Wu, N.; Luo, C.; Liu, Y.; Li, N.; Xie, C.; Cao, G.; Ye, C.; Wang, H. Prediction of liquid holdup in horizontal gas wells based on dimensionless number selection. *J. Energy Resour. Technol.* **2023**, *145*, 113001. [[CrossRef](#)]
7. Liu, Y.; Ozbayoglu, E.; Upchurch, E.; Baldino, S. Computational fluid dynamics simulations of Taylor bubbles rising in vertical and inclined concentric annuli. *Int. J. Multiph. Flow* **2023**, *159*, 104333. [[CrossRef](#)]
8. Brito, R.; Pereyra, E.; Sarica, C. Effect of well trajectory on liquid removal in horizontal gas wells. *J. Petrol. Gas Sci. Eng.* **2017**, *156*, 1–11. [[CrossRef](#)]
9. Yuan, G.; Dwivedi, P.; Kwok, C. The impact of increase in lateral length on production performance of horizontal shale wells. In Proceedings of the SPE Europe Featured at 79th Eage Conference and Exhibition, Paris, France, 13–14 June 2017.
10. Liu, Y.; Luo, C.; Zhang, L.; Liu, Z.; Xie, C.; Wu, P. Experimental and modeling studies on the prediction of liquid loading onset in gas wells. *J. Nat. Gas Sci. Eng.* **2018**, *57*, 349–358. [[CrossRef](#)]
11. Zhang, L.; Luo, C.; Liu, Y.; Zhao, Y.; Xie, C.; Xie, C. A simple and robust model for prediction of liquid-loading onset in gas wells. *Int. J. Oil Gas Coal Technol.* **2021**, *26*, 245–263. [[CrossRef](#)]
12. Lockhart, R.W.; Martinelli, R.C. Proposed Correlation of Data for Isothermal Two-Phase, Two-Component Flow in Pipes. *Chem. Eng. Prog.* **1949**, *45*, 38–48.
13. Taitel, Y.; Dukler, A.E. A theoretical approach to the Lockhart-Martinelli correlation for stratified flow. *Int. J. Multiph. Flow* **1976**, *2*, 591–595. [[CrossRef](#)]
14. Taitel, Y.; Dukler, E.A. A model for predicting flow regime transitions in horizontal and near horizontal gas-liquid flow. *AIChE J.* **1976**, *22*, 47–55. [[CrossRef](#)]
15. Hart, J.; Hamersma, P.J.; Fortuin, J.M.H. Correlations predicting frictional pressure drop and liquid holdup during horizontal gas-liquid pipe flow with a small liquid holdup. *Int. J. Multiph. Flow* **1989**, *15*, 947–964. [[CrossRef](#)]
16. Grolman, E.; Fortuin, J.M. Gas-liquid flow in slightly inclined pipes. *Chem. Eng. Sci.* **1997**, *52*, 4461–4471. [[CrossRef](#)]
17. Chen, X.T.; Cai, X.D.; Brill, J.P. Gas-Liquid Stratified-Wavy Flow in Horizontal Pipelines. *ASME J. Energy Res. Tech.* **1997**, *119*, 4. [[CrossRef](#)]

18. Al-Safran, E. *An Experimental and Theoretical Investigation of Slug Flow Characteristics in the Valley of a Hilly-Terrain Pipeline*; The University of Tulsa: Tulsa, OK, USA, 2003.
19. Langsholt, M.; Holm, H. Liquid accumulation in gas-condensate pipelines—An experimental study. In Proceedings of the 13th International Conference on Multiphase Production Technology, Edinburgh, UK, 13–15 June 2007.
20. Fan, Y.; Wang, Q.; Zhang, H.; Danielson, T.J.; Sarica, C. A model to predict liquid holdup and pressure gradient of near-horizontal wet-gas pipelines. *SPE Proj. Facil. Constr.* **2007**, *2*, 1–8. [[CrossRef](#)]
21. Zhang, H.Q.; Sarica, C. A model for wetted-wall fraction and gravity center of liquid film in gas/liquid pipe flow. *SPE J.* **2011**, *16*, 3. [[CrossRef](#)]
22. Alsaadi, Y.; Pereyra, E.; Torres, C.; Sarica, C. Liquid loading of highly deviated gas wells from 60° to 88°. In Proceedings of the SPE Annual Technical Exhibition, Houston, TX, USA, 28–30 September 2015.
23. Fan, Y.; Pereyra, E.; Torres, C.; Andin, T.; Sarica, C. Experimental study on the onset of intermittent flow and pseudo-slug characteristics in upward inclined pipes. In Proceedings of the 17th International Conference on Multiphase Production Technology, Cannes, France, 10–11 June 2015.
24. Fan, Y.; Pereyra, E.; Sarica, C. Onset of liquid film reversal in upward-inclined pipe. *SPE J.* **2018**, *23*, 1630–1647. [[CrossRef](#)]
25. Arabi, A.; Salhi, Y.; Bouderval, A.; Zenati, Y.; Si-Ahmed, E.K.; Legrand, J. Onset of intermittent flow: Visualization of flow structures. *Oil Gas Sci. Technol.—Rev. D'Ifp Energ. Nowv.* **2021**, *76*, 27. [[CrossRef](#)]
26. Karami, H.; Torres, C.F.; Pereyra, E.; Sarica, C. Experimental investigation of Three-Phase Low Liquid Loading Flow. *Oil Gas Facil.* **2016**, *5*, 45–56. [[CrossRef](#)]
27. Vuong, D. Pressure Effects on Two-Phase Oil-Gas Low-Liquid Loading Flow in Horizontal Pipes. Ph.D. Dissertation, The University of Tulsa, Tulsa, OK, USA, 2016.
28. Rodrigues, H. Pressure Effects on Low-Liquid Loading Two-Phase Flow in Near-Horizontal upward Inclined Pipes. Ph.D. Dissertation, The University of Tulsa, Tulsa, OK, USA, 2018.
29. Soedarmo, A.; Pereyra, E.; Sarica, C. Gas-liquid flow in an upward inclined large diameter pipe under elevated pressures. In Proceedings of the Offshore Technology Conference, Houston, TX, USA, 8–10 May 2019.
30. Farokhpour, R.; Liu, L.; Langsholt, M.; Hald, K.; Amundsen, J.; Lawrence, C. Dimensional analysis and scaling in two-phase gas-liquid stratified pipe flow-Methodology evaluation. *Int. J. Multiph. Flow* **2020**, *122*, 103139. [[CrossRef](#)]
31. Al-Sarkhi, A.; Sarica, C. Power-law correlation for two-phase pressure drop of gas-liquid flows in horizontal pipelines. *SPE Prod. Facil.* **2010**, *5*, 176–182. [[CrossRef](#)]
32. Luo, C.; Wu, N.; Dong, S.; Liu, Y.; Ye, C.; Yang, J. Experimental and modeling studies on pressure gradient prediction for horizontal gas wells based on dimensionless number analysis. In Proceedings of the SPE Annual Technical Conference and Exhibition, Dubai, United Arab Emirates, 21–23 September 2021.
33. Al-Sarkhi, A.; Duc, V.; Sarica, C.; Pereyra, E. Upscaling modeling using dimensional analysis in gas-liquid annular and stratified flows. *J. Petrol. Gas Sci. Eng.* **2016**, *137*, 240–249. [[CrossRef](#)]
34. Nair, J.V. Gas Lift Application and Severe Slugging in Toe Down Horizontal Wells. Ph.D. Dissertation, The University of Tulsa, Tulsa, OK, USA, 2017.
35. Arabi, A.; Salhi, Y.; Zenati, Y.; Si-Ahmed, E.K.; Legrand, J. A discussion on the relation between the intermittent flow sub-regimes and the frictional pressure drop. *Int. J. Heat Mass Transf.* **2021**, *181*, 121895. [[CrossRef](#)]
36. Mandhane, J.; Gregory, G.; Aziz, K. A flow pattern map for gas-liquid flow in horizontal pipes. *Int. J. Multiph. Flow* **1974**, *1*, 537–553. [[CrossRef](#)]
37. Zhang, H.; Wang, Q.; Sarica, C.; Brill, J. Unified model for gas-liquid pipe flow via slug dynamics—part 1: Model development. *J. Energy Resour. Technol.* **2003**, *125*, 274–283. [[CrossRef](#)]
38. Andritsos, N.; Hanratty, T. Influence of interfacial waves in stratified gas-liquid flows. *AIChE J.* **1987**, *33*, 444–454. [[CrossRef](#)]
39. Beggs, D.; Brill, B. A Study of Two-phase flow in inclined pipes. *J. Pet. Technol.* **1973**, *25*, 607–617. [[CrossRef](#)]
40. Mukherjee, H.; Brill, J. Liquid holdup correlations for inclined two-phase flow. *J. Pet. Technol.* **1983**, *22*, 1003–1008. [[CrossRef](#)]
41. Lou, W.; Wang, Z.; Li, P.; Sun, X.; Sun, B.; Liu, Y.; Sun, D. Wellbore drift flow relation suitable for full flow pattern domain and full dip range. *Petrol. Explor. Dev.* **2022**, *49*, 694–706. [[CrossRef](#)]
42. Luo, C.; Zhang, L.; Liu, Y.; Zhao, Y.; Xie, C.; Wang, L.; Wu, P. An improved model to predict liquid holdup in vertical gas wells. *J. Petrol. Sci. Eng.* **2020**, *184*, 349–358. [[CrossRef](#)]
43. Liu, Y.; Tong, T.; Ozbayoglu, E.; Yu, M.; Upchurch, E. An improved drift-flux correlation for gas-liquid two phase flow in horizontal and vertical upward inclined wells. *J. Petrol. Sci. Eng.* **2020**, *195*, 1–14. [[CrossRef](#)]
44. Eaton, B.; Knowles, C.; Silberberg, H. The prediction of flow patterns, liquid holdup and pressure losses occurring during continuous two-phase flow in horizontal pipelines. *J. Pet. Technol.* **1967**, *19*, 815–828. [[CrossRef](#)]
45. Xiao, J.; Shoham, O.; Brill, J. A comprehensive mechanistic model for two-phase flow in pipelines. In Proceedings of the SPE Annual Technical Conference and Exhibition, New Orleans, LA, USA, 23–26 September 1990.

**Disclaimer/Publisher's Note:** The statements, opinions and data contained in all publications are solely those of the individual author(s) and contributor(s) and not of MDPI and/or the editor(s). MDPI and/or the editor(s) disclaim responsibility for any injury to people or property resulting from any ideas, methods, instructions or products referred to in the content.